

pubs.acs.org/NanoLett Letter

Phonon-Mediated Interlayer Charge Separation and Recombination in a MoSe₂/WSe₂ Heterostructure

Zilong Wang, Patrick Altmann, Christoph Gadermaier, Yating Yang, Wei Li, Lavinia Ghirardini, Chiara Trovatello, Marco Finazzi, Lamberto Duò, Michele Celebrano, Run Long, Deji Akinwande, Oleg V. Prezhdo,* Giulio Cerullo,* and Stefano Dal Conte*



Cite This: Nano Lett. 2021, 21, 2165-2173



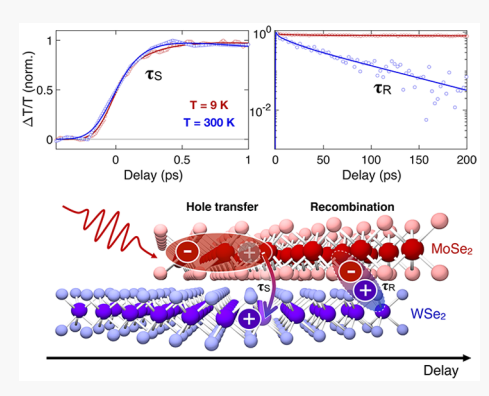
ACCESS

Metrics & More

Article Recommendations

s Supporting Information

ABSTRACT: Monolayer transition metal dichalcogenides bear great potential for photodetection and light harvesting due to high absorption coefficients. However, these applications require dissociation of strongly bound photogenerated excitons. The dissociation can be achieved by vertically stacking different monolayers to realize band alignment that favors interlayer charge transfer. In such heterostructures, the reported recombination times vary strongly, and the charge separation and recombination mechanisms remain elusive. We use two color pump—probe microscopy to demonstrate that the charge separation in a MoSe₂/WSe₂ heterostructure is ultrafast (~200 fs) and virtually temperature independent, whereas the recombination accelerates strongly with temperature. Ab initio quantum dynamics simulations rationalize the experiments, indicating that the charge separation is temperature-independent because it is barrierless, involves dense acceptor states, and is promoted by higher-frequency out-of-plane vibrations. The



strong temperature dependence of the recombination, on the other hand, arises from a transient indirect-to-direct bandgap modulation by low-frequency shear and layer breathing motions.

KEYWORDS: 2D Heterostructure, femtosecond pump-probe spectroscopy, charge transfer, transition metal dichalcogenides, TDDFT

emiconducting transition metal dichalcogenides (TMDs) are layered materials in which each layer consists of a hexagonal lattice of transition metal atoms (M, typically Mo or W) embedded between two hexagonal lattices of chalcogen atoms (X, usually S or Se), in MX₂¹ proportions. Since the layers are held together by weak van der Waals interactions, they can be easily thinned down to a monolayer (ML). The exceptionally high absorption coefficient in TMDs, combined with good chemical stability and a variety of scalable fabrication techniques, holds promise for electronic, optoelectronic, photonic and light-harvesting applications.² TMDs feature a direct bandgap, and their optical properties are dominated by excitons (Coulombically bound electron-hole pairs) with large binding energies (\sim 0.5 eV), promoted by the two-dimensional quantum confinement and by the reduced dielectric screening.

For photodetection and light-harvesting applications, it is imperative to efficiently dissociate the photogenerated excitons and to prevent recombination of the charges for a time long enough to extract them from the device or allow them to catalyze a photochemical reaction. While the electrons and holes in indirect bandgap semiconductors quickly relax into separate band extrema with sufficiently different wave vectors to slow down recombination (~ns), in direct bandgap semiconductors, such as ML-TMDs, electron—hole recombi-

nation is fast (i.e., few ps at cryogenic temperatures).^{8,9} A common solution to prolong carrier lifetime is to interface two different ML-TMDs to form a vertical heterostructure (HS). Since the two materials are held together by weak van der Waals forces, they largely preserve their individual electronic structures. Unlike HS of conventional semiconductors, they do not suffer from lattice mismatch constraints, enabling a very large number of combinations.

Among the different HS, the most interesting for applications are those characterized by a type II, or staggered, band alignment, shown in Figure 1a, where the valence band maximum and the conduction band minimum lie in different layers. This configuration makes it energetically favorable for the photoexcited electrons to be on one semiconductor layer and for the holes to be on the other, promoting ultrafast charge separation. Type II HS enable efficient photodetectors, solar cells 23,24 and photocatalysts. Upon

Received: December 16, 2020 Revised: February 9, 2021 Published: February 16, 2021





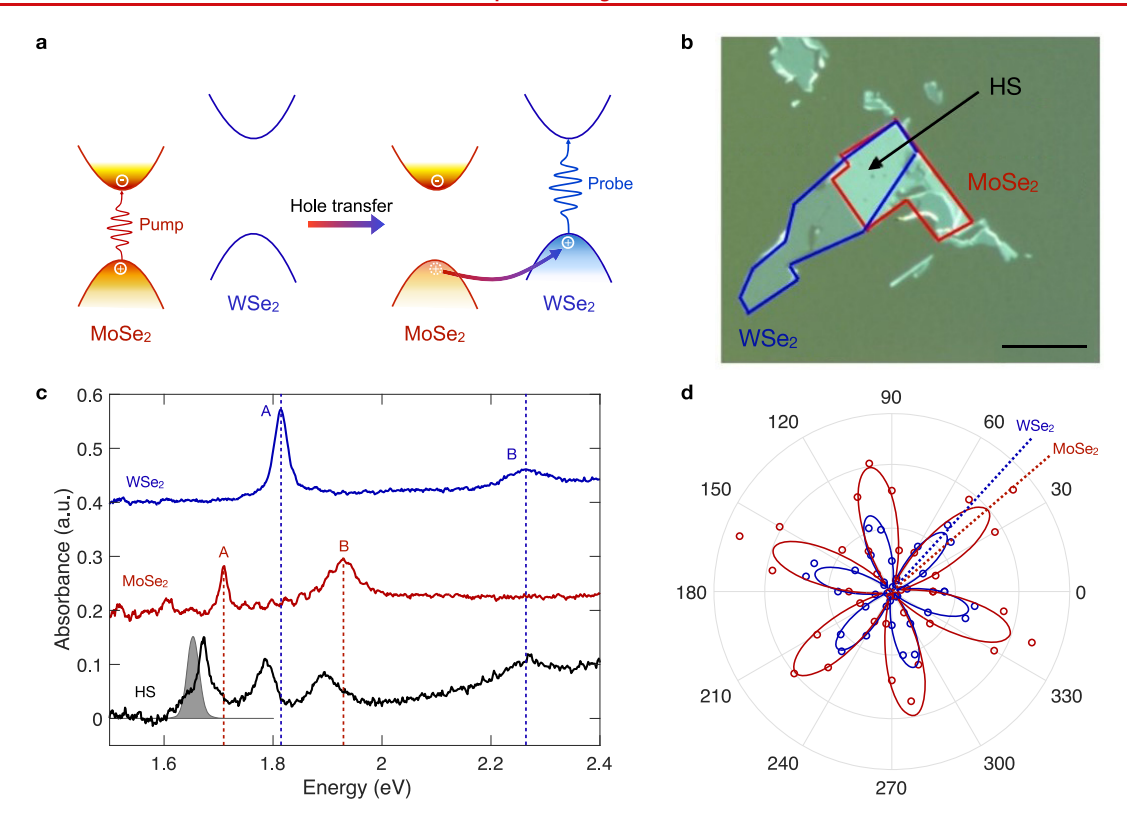


Figure 1. Equilibrium optical properties of the $MoSe_2/WSe_2$ HS. (a) Scheme of the theoretically predicted valence and conduction band alignment at the K/K' points. The arrow represents the IL hole transfer process. (b) Optical microscope image of the HS. The scale bar is $10 \ \mu m$. (c) Absorption spectra at $T = 9 \ K$ of ML-MoSe₂ (red), ML-WSe₂ (blue), and their HS (black). The gray trace is the spectrum of the pump pulse. (d) Angle-dependent second harmonic generation for the evaluation of the twist angle between the layers.

photoexcitation, intralayer excitons formed in one layer efficiently separate via charge transfer on a subpicosecond time scale, resulting in the formation of interlayer (IL) excitons for which the electron and hole reside in different layers. IL excitons are characterized by recombination times several orders of magnitude longer than the intralayer excitons, that is, up to hundreds of nanoseconds. Pecause of these long recombination times, IL excitons can diffuse over micrometer lengths and retain spin/valley polarization, giving rise to pure spin/valley diffusion currents. Phe IL twist angle constitutes an additional tuning knob for IL excitons, as confirmed by the recent observation of Moiré trapped excitons in magic-angle twisted TMD-HS.

Time-domain spectroscopies (i.e., transient absorption and time-resolved photoluminescence) have been extensively used to study charge separation and recombination dynamics in TMD-HS. Transient absorption experiments performed on HS with different stacking sequences show that the ultrafast separation time $\tau_{\rm S}$ does not depend appreciably on the twist angle $\Delta\phi$ between the crystal axes of the two MLs. Is, In contrast, the carrier recombination time $\tau_{\rm R}$ for the MoSe₂/WSe₂ HS shows a strong non-monotonic dependence on $\Delta\phi$; however, a systematic study of both the radiative and nonradiative recombination processes and their dependence on $\Delta\phi$, the layer stacking sequence, and possibly the dielectric environment of the HS is missing.

IL exciton emission has been mainly studied in the MoSe₂/WSe₂ HS showing a progressive intensity quenching and a strong decrease of the decay time upon increasing temperatures.²⁹ This suggests that the IL recombination process is mainly driven by temperature-dependent relaxation channels.

IL carrier dynamics has been simulated by different theoretical models, ^{40–47} predicting an IL charge separation time ranging from a few tens of femtoseconds to 1–2 ps for different types of HS. Several mechanisms have been proposed to explain the rapid and efficient IL charge transfer in TMD-HS, including the presence of an excitation-induced interfacial dipole, ⁴⁰ phonon-mediated scattering processes, ^{43,48} and a coherent mixing between donor and acceptor states. ⁴² On the contrary, a theoretical modeling of the carrier recombination dynamics and an explanation of its temperature dependence are still lacking.

Here we use two-color femtosecond transient absorption microscopy to study the temperature dependence of the charge transfer and recombination dynamics in a MoSe₂/WSe₂ HS (see the sketch in Figure 1a). We time-resolve a nearly temperature-independent 200 fs charge separation time and a strongly temperature-dependent recombination time, which varies by 2 orders of magnitude between room temperature (RT) and 9 K. Ab initio quantum dynamics simulations rationalize our findings, demonstrating that the energy lost during the charge separation and recombination processes is accommodated by the relatively high-frequency out-of-plane lattice vibrations, which create a nonadiabatic coupling between the states localized across the interface and cannot be thermally activated within the experimental temperature range. These simulations confirm that the hole transfer is ultrafast and temperature independent, because it is energetically favorable and leads to a dense manifold of acceptor states. On the other hand, the charge recombination process depends on temperature, since it is promoted by heat-activated lowfrequency shear and layer breathing modes. These phonon

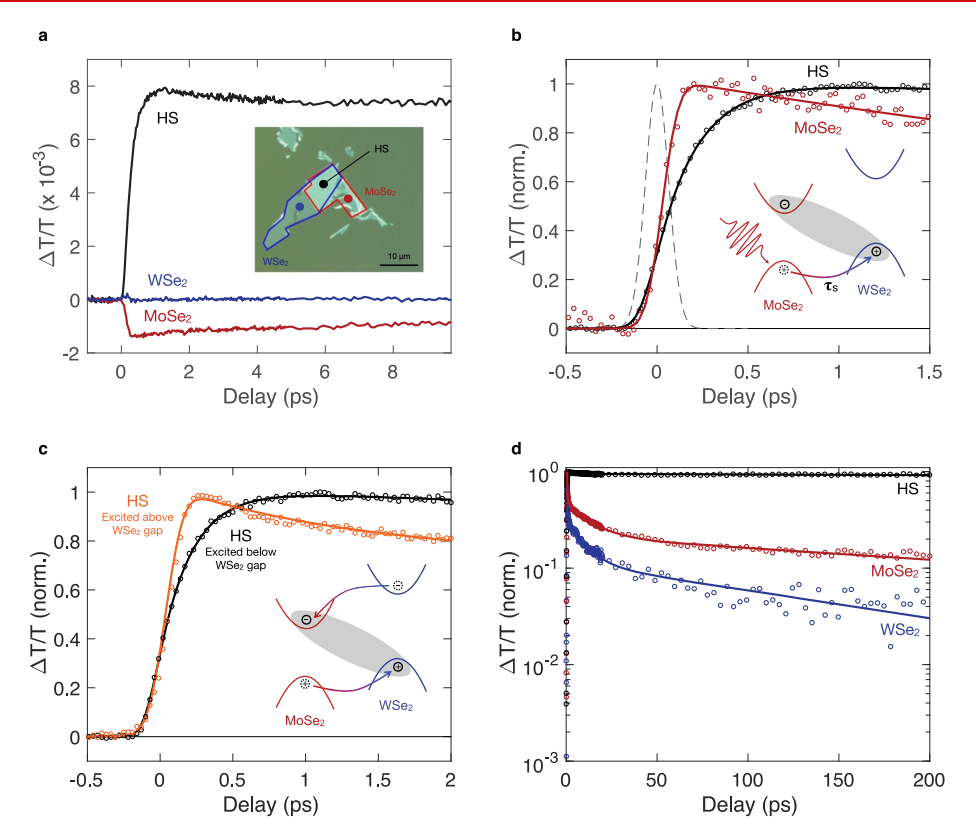


Figure 2. Charge transfer dynamics in MoSe₂/WSe₂ HS at T=9 K. (a) $\Delta T/T$ temporal traces measured at the WSe₂ A exciton resonance on the MoSe₂/WSe₂ HS (black) and the isolated MoSe₂ (red), WSe₂ (blue) layers, upon optical excitation resonant with the optical band gap of MoSe₂ (1.69 eV). The incident pump fluence is $70 \, \frac{\mu J}{\text{cm}^2}$. (b) Comparison between the build-up dynamics of the $\Delta T/T$ traces of the HS and MoSe₂ (both traces are normalized for a better comparison). The maximum variation of the signal measured on the HS is clearly delayed with respect to the one of the MoSe₂ because of the finite hole transfer time. The continuous lines are fits to the data. (c) Comparison between $\Delta T/T$ response of the HS for layer (black) and non layer-selective (orange) photoexcitation (i.e., pump energy below (1.69 eV) and above (2.07 eV) the optical gap of MoSe₂). In the latter case, the signal exhibits an instantaneous build-up time as for the isolated TMD layers. (d) Long delay dynamics at the energy of the WSe₂ A exciton measured on the HS excited with pump photon energy of 1.69 eV compared with the A exciton resonance measured on the isolated MoSe₂ and WSe₂ layers (pump photon energy at 2.07 eV). Continuous lines are fits to the data with a double exponential decay function. The longer decay constant extracted from the fit is 470 ps (MoSe₂) and 180 ps (WSe₂), while it becomes >3 ns for the HS.

modes periodically modulate the band structure of the HS, which bears an indirect gap at equilibrium, and generate a transient direct gap which greatly enhances both the radiative and nonradiative recombination rate of the IL exciton. The unique combination of experiments and *ab initio* simulations and their very good agreement clarify the microscopic mechanisms underlying the charge separation and recombination processes.

RESULTS AND DISCUSSION

The MoSe₂/WSe₂ HS, shown in Figure 1b, was prepared using mechanical exfoliation and transferred onto a fused silica substrate (see Supporting Information). The technique yields ML flakes with a typical lateral size of 30 μ m and an ~10 × 10 μ m² overlap region when deposited one on top of the other. Figure 1c displays the absorption spectra of the HS and of the individual MLs, measured by white light microscopy at the temperature T=9 K. The MLs show the characteristic A and B absorption resonances ascribed to electronic transitions at the K and K' points, yielding excitons consisting of an electron in the conduction band (CB) and a hole in the spin—orbit split valence band (VB), bound together by Coulomb attraction. MoSe₂ has a lower bandgap with the A exciton peaking at 1.70 eV as compared to 1.81 eV for the A exciton of WSe₂ (see

Figure 1c). The absorption spectrum of the HS shows the A and B resonances of both MoSe2 and WSe2, including their doping-induced shoulders. All peaks are red-shifted compared to their position in the ML due to the modified dielectric environment.⁴⁹ In the HS, the A excitonic resonances of MoSe₂ and WSe₂ redshift by ~35 and ~25 meV, respectively. Coupling between the two layers leads to a shift of the band gap and the exciton binding energy via increased dielectric screening but not to the creation of qualitatively different electronic states around the K and K' points, confirming that the electronic structure of the individual MLs is well retained in the HS due to the weak van der Waals coupling. The twist angle $\Delta \phi$ between the two MLs was measured via polarizationdependent second harmonic generation (SHG) and found to be $\Delta \phi \approx 54^{\circ}$ (see Figure 1d and Figure S4 in the Supporting Information).

To visualize in real time the charge separation and recombination processes in the HS, we employ two-color femtosecond transient absorption microscopy. In this technique, the sample is photoexcited by an ultrashort laser pulse (the pump) and the differential transmission $(\Delta T/T)$ is measured by a time-delayed laser pulse (the probe) with a different photon energy with respect to the pump. Because of the small size of the HS and the need to spatially resolve its

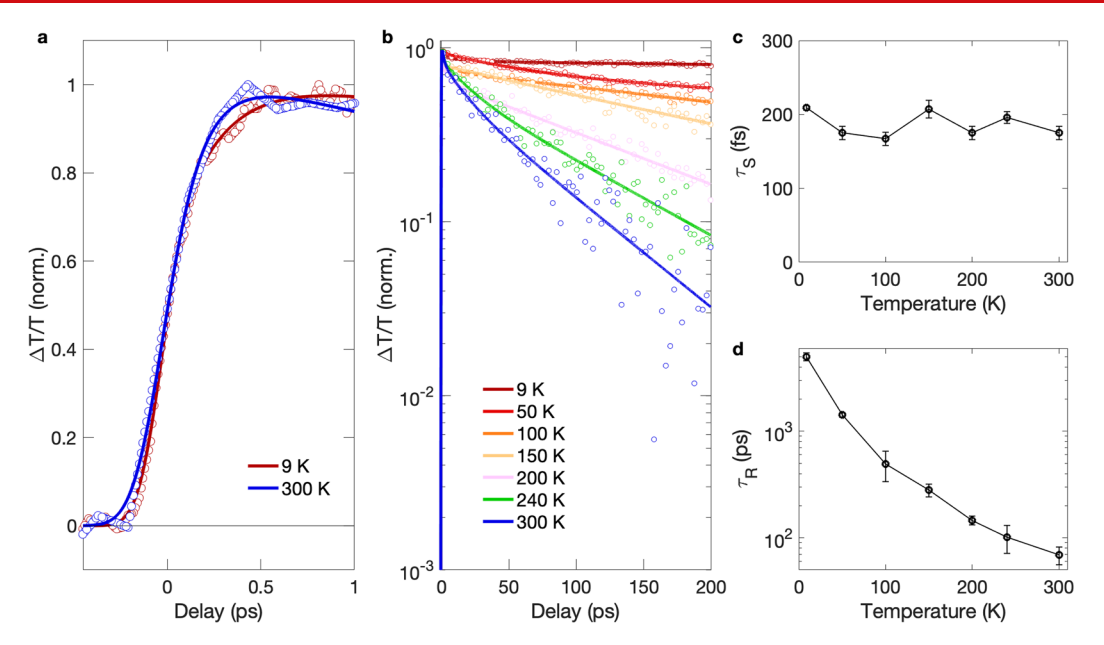


Figure 3. Temperature-dependent exciton dissociation and recombination dynamics. (a) Early delay time $\Delta T/T$ dynamics measured on the HS for pump at 1.67 eV and probe at 1.78 eV for different sample temperatures (open symbols) and fits of the build-up dynamics (continuous lines). (b) Relaxation dynamics measured at different temperatures (open symbols) and fits to a double-exponential decay (continuous lines). (c) Charge separation time extracted from the fit function in (a) at different temperatures. (d) τ_R as a function of the temperature. τ_R is the longer decay constant extracted from a double exponential fit of the temporal traces.

 $\Delta T/T$ signal and distinguish it from those of the neighboring MLs, pump and probe pulses have been collinearly combined into a home-built microscope (see Figure S2 in the Supporting Information), allowing a spatial resolution of ~5 μ m.

Figure 2a shows two-color $\Delta T/T$ time traces, measured at T= 9 K with the pump pulse tuned at 1.65 eV, slightly below the MoSe₂ A exciton of the HS, and the probe pulse tuned at 1.77 eV, in resonance with the A exciton of WSe2. Under these conditions, only MoSe2 is excited, while the pump photon energy falls below the WSe2 bandgap. For the MoSe2 ML (red trace in Figure 2a), we observe a weak negative signal ($\Delta T/T$ < 0) which rises instantaneously within the 150 fs instrumental response function (IRF) of the apparatus. Since the 1.77 eV probe photon energy is slightly below the B exciton peak in MoSe₂ (located at 1.87 eV), we assign this signal to a rigid redshift of the B exciton resonance due to bandgap renormalization (BGR) induced by the carriers photogenerated by the pump pulse. 50 The observation of an instantaneous BGR upon photoexcitation is in agreement with several previous studies on other TMDs. 50,51,53 Moving to the WSe2 ML (blue trace in Figure 2a), except for a weak signal around time zero due to nonresonant pump-probe interactions we observe no $\Delta T/T$ signal at longer delays; this is expected because the pump photon energy lies well below the bandgap of WSe₂ and the fluence is low enough that multiphoton excitation can be neglected. When moving to the HS (black trace in Figure 2a) the signal changes dramatically: we observe an intense positive $\Delta T/T$ signal which does not rise instantaneously but with a clearly resolved delay. We interpret this signal as due to Pauli blocking of the A exciton transition in WSe2 from holes in the VB of WSe2 which have been injected following charge transfer from the VB of MoSe₂ and IL exciton formation.

Figure 2b compares the normalized $\Delta T/T$ dynamics for MoSe₂ and for the HS, measured at T=9 K. In order to visually capture their different build-up times the MoSe₂

dynamics has been flipped in sign. It is evident that the HS signal has a delayed build-up which is well resolved by our experiment; fitting the process with an exponential rise, convoluted with the IRF (i.e., the cross-correlation of the pump and probe pulse intensity profiles with a full width at half-maximum of 150 fs) yields a time constant $\tau_S = 200 \pm 20$ fs for the charge separation process. This result is in a good agreement with previous studies on similar TMD HS, which found τ_S of the same order of magnitude and showed it to be independent of twist angle.¹⁸ By tuning the pump photon energy above the optical gap of WSe₂, the $\Delta T/T$ signal (orange curve in Figure 2c) shows a pulse-width limited buildup dynamics, comparable to the one measured in the isolated TMD layers. The change of the rise time is a consequence of the lack of layer selectivity for the photoexcitation: at increasing pump photon energy, the pump pulse creates excitons also in the WSe2 layer of the HS. This results in an instantaneous bleaching signal measured at the A excitonic transition of WSe₂. Creation of intralayer excitons in both of the TMD layers opens up new scattering channels for the photoexcited carriers, giving rise to a fast electron transfer from WSe₂ to MoSe₂ resulting in a subpicosecond decay component.

Figure 2d shows the dynamics of the HS at 9 K on a longer time scale. The positive $\Delta T/T$ signal shows an initial decay by a few percent on a few-picosecond time scale, followed by a slow exponential decay with a time constant τ_R of several nanoseconds. As a comparison, we show the decay of the A exciton photobleaching signal in ML-WSe2 and ML-MoSe2 when the photoexcitation is tuned above their bandgaps to 2.07 eV (blue line in Figure 2d); in this case, the signal features a much faster and multiexponential decay. As expected, the IL excitons in the HS recombine much more slowly than the intralayer excitons in the ML. 14,27

Having identified a clear spectral signature of the IL exciton dynamics in the HS, we set out to investigate the temperature

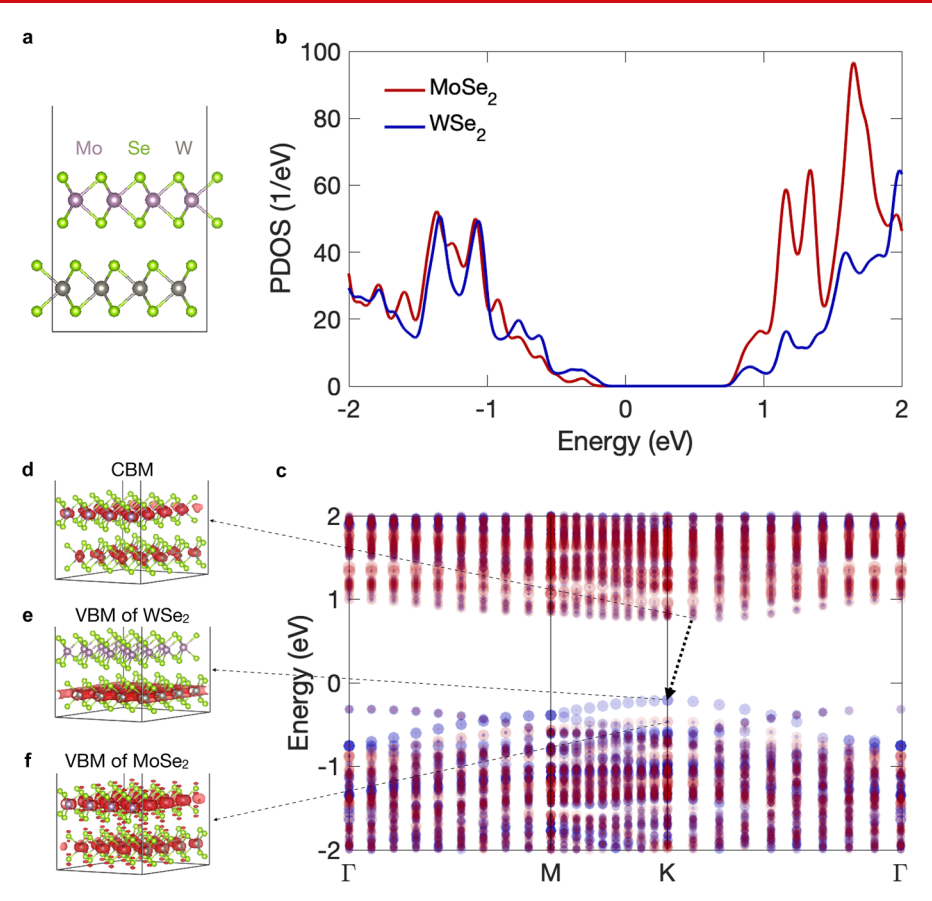


Figure 4. Simulated MoSe₂/WSe₂ HS and its electronic properties. (a) Geometric structure of the simulation cell. (b) Projected density of states (PDOS) of the MoSe₂/WSe₂ HS obtained with PBE+SOC. Thirty k-points from Γ to M to K to Γ are sampled with 10 k-points between each pair. (c) Projected band structure corresponding to the PDOS in part (b). The arrow indicates the indirect bandgap. (d–f) Charge densities for conduction band minimum (CBM), and VBM of WSe₂ and VBM of MoSe₂, respectively.

dependence of its formation and decay processes. Figure 3a compares the IL exciton build-up process measured at 9 K and at RT; the dynamics appear similar with only a slight speed-up observed in the RT data. This is confirmed by performing a temperature dependence of the IL exciton formation process and extracting a charge separation time constant τ_s (Figure 3c) which is nearly independent of temperature. We stress that such temperature-independent $\tau_{\rm S}$ has been previously observed in a WS₂/WSe₂ HS and found to be shorter than the 60 fs time resolution of the setup used for that study.⁵² Figure 3b reports the temperature dependence of the IL exciton recombination process, measured up to 200 ps time scale due to experimental limitations. We stress that for the temperature range explored in the experiment, a double exponential decay model provides a better fit to the dynamics than a single exponential one. While the fast decay component slightly depends on the temperature, the slower one (τ_R) displays a stronger dependence with the temperature going from $\tau_R = 5 \pm 0.4$ ns at 9 K to $\tau_{\rm R}$ = 80 ± 10 ps at RT. Figure 3d shows the time constants extracted from the fit of the time traces. The strong temperature dependence of τ_R is related to the drastic reduction of the IL exciton radiative recombination time, previously observed with time-resolved photoluminescence on the same type of HS and not understood.^{28,29}

In order to rationalize the observed temperature dependences of the IL exciton formation and recombination processes, we carried out *ab initio* quantum dynamics simulations combining real-time time-dependent density

functional theory and nonadiabatic molecular dynamics. 54-56 The simulations are performed on the MoSe₂/WSe₂ HS shown in Figure 4. The band structure calculations show, in agreement with previous results, 57,58 that the $MoSe_2/WSe_2$ HS has an indirect bandgap. Because the MoSe₂ VB maximum (VBM) is inside the WSe₂ VB, the MoSe₂ VBM couples and mixes with multiple WSe₂ states (see Figure 4c), such that the initial state for the hole transfer process can be delocalized between the two layers, facilitating ultrafast charge transfer across the weakly coupled van der Waals HS. 42,59 Figure 5a shows the calculated buildup of the hole population in WSe₂, following selective excitation of MoSe2. The hole transfer is ultrafast and independent of temperature (see Figure 5b), because it is energetically favorable and is characterized by a high density of final states in the dense manifold of WSe2 VB states, and because it is promoted by TMDs out-of-plane motions⁶⁰ with frequencies around 240–250 cm⁻¹ (see Figure S5a in the Supporting Information). Phonons at such frequencies cannot be thermally activated within the experimental temperature range, since 250 cm⁻¹ corresponds to ~360 K in agreement with the observed temperature independence of the charge separation process. Rapid nonadiabatic transition from the MoSe₂ VBM to WSe₂ VB states immediately below in energy localizes the holes within WSe2, resulting in an ultrafast transfer. Longer time scale ab initio quantum dynamics simulations, Figure 5c,d, also support the experimental results for the IL exciton recombination. Similar to the experiments, the simulations show a strong

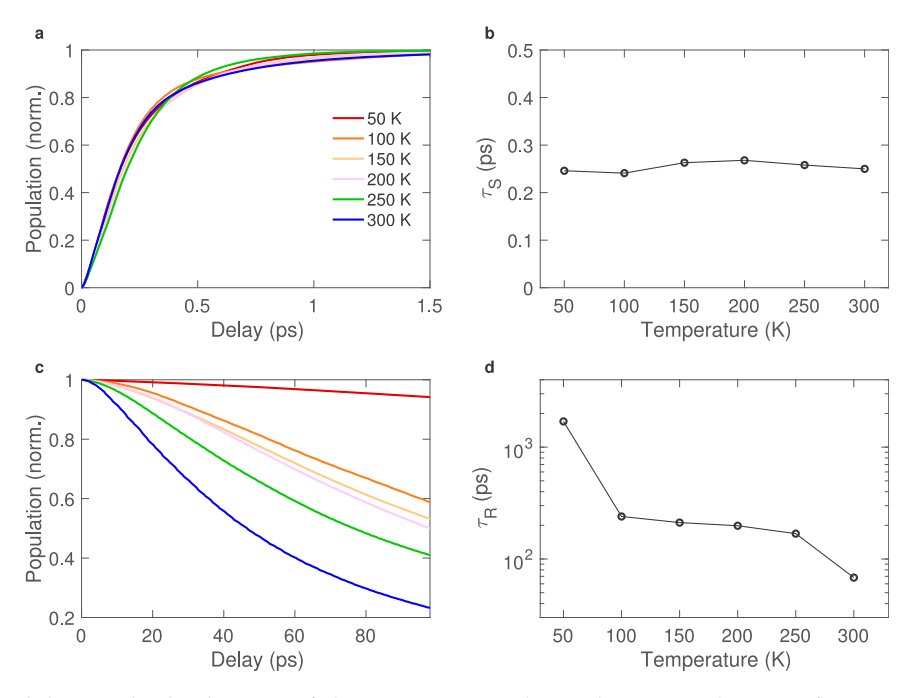


Figure 5. Ab initio nonadiabatic molecular dynamics of charge separation and recombination in the MoSe₂/WSe₂ HS. (a) Evolution of hole population on the WSe₂ layer at different temperatures. (b) Hole transfer time versus temperature. Hole transfer is rapid and independent of temperature because it occurs within a dense manifold of states and is driven by the same high-frequency phonon, Figure S2. (c) Decay of population of the IL exciton over time due to nonradiative electron—hole recombination at different temperatures. The decay slows down considerably at lower temperatures due to decreased nonadiabatic electron—phonon coupling and increased band gap, Table S1. (d) Temperature dependence of the calculated recombination time.

temperature dependence of the charge recombination with the time scale ranging from over 1 ns at 50 K to under 100 ps at 300 K (see Table S1 in the Supporting Information). Just as for the hole transfer, the electronic energy lost during the recombination is deposited into the out-of-plane TMD motions in the 240-250 cm⁻¹ frequency range (Figure S5b in the Supporting Information). These modes cannot be thermally activated within the considered temperature range, and therefore the temperature dependence arises from another source. In particular, the MoSe₂/WSe₂ HS has an indirect bandgap (see Figure 4c), but the energy difference to the direct bandgap is small, around 10 meV. The atomistic simulations show that low frequency motions of the MoSe₂/WSe₂ HS, such as the shear (18 cm⁻¹) and layer breathing (29 cm⁻¹) modes,60 perturb the bilayer geometry, frequently turning it into a direct bandgap material and allowing charge recombination without a variation of crystal momentum. These slow vibrations with frequencies corresponding to 25-40 K are activated thermally within the studied temperature range, rationalizing the observed behavior. Contrary to its strong temperature dependence, τ_R is largely independent of the excitation fluence (see Figure S3 in the Supporting Information) and hence of the exciton or charge density. This suggests that the electron-hole pair after separation remain paired in an IL exciton and eventually recombine with each other (geminate recombination), resulting in dynamic behavior that is independent of the excitation density. If, on the other hand, the separated charges diffused inside the MLs until a nongeminate recombination occurs, one would instead observe a higher recombination rate for higher excitation fluences. This fluence independence confirms our assignment of τ_R to the IL exciton recombination and rules out the most important alternative assignments. Our data show that a significant

fraction of all initially excited carriers recombines via this process, which dominates the dynamics in the temporal window between 30 and 200 ps. This does not, however, exclude the presence of other recombination pathways, which may even be dominant on a slower time scale. Both the Shockley–Read–Hall mechanism and Auger recombination would display only a weak temperature dependence and a decreasing recombination rate at higher fluences. Similarly, we can exclude the dominant role of dark excitons in the recombination dynamics because they would give rise to a recombination rate decreasing with temperature, as observed in Se-based TMDs, where dark excitons are energetically lower lying with respect to the bright ones. 62

CONCLUSIONS

In conclusion, we have employed ultrafast transient absorption microscopy to study the temperature-dependent IL charge separation and recombination process in a MoSe₂/WSe₂ HS. We have resolved the charge separation dynamics with a time constant $\tau_s = 200 \pm 20$ fs and found that this time constant is virtually independent of temperature. On the other hand, the recombination time constant τ_R displays a strong temperature dependence, becoming progressively shorter at higher temperatures. Ab initio quantum dynamics simulations reproduce the experimental data very well and shed light on the underlying physical processes. They demonstrate that the energy lost by the charges during the photoinduced charge separation and recombination is accommodated by the relatively highfrequency out-of-plane TMD vibrations that create a nonadiabatic coupling between the states localized across the interface. Since the activation temperature of these phonon modes is higher than the experimental temperature range, the hole transfer process is temperature independent. The charge

recombination, on the other hand, depends on temperature, because thermally activated low-frequency phonon modes transiently modulate the system geometry and bring the heterojunction from an indirect bandgap to a direct bandgap, allowing recombination without variation of crystal momentum. The good agreement between theory and experiment allows us to generalize our approach to other materials and indicates that the time-domain simulations can be used to design novel HS with higher charge separation efficiency and improved performances.

ASSOCIATED CONTENT

Solution Supporting Information

The Supporting Information is available free of charge at https://pubs.acs.org/doi/10.1021/acs.nanolett.0c04955.

Details of heterostructure preparation and characterization; description of transient absorption microscopy measurements; dependence of build-up and relaxation dynamics on excitation power; polarization-dependent SHG measurements; details and additional results of time-domain *ab initio* simulations (PDF)

AUTHOR INFORMATION

Corresponding Authors

Oleg V. Prezhdo — Department of Chemistry, University of Southern California, Los Angeles, California 90089, United States; IFN-CNR, I-20133 Milano, Italy; orcid.org/ 0000-0002-5140-7500; Email: prezhdo@usc.edu

Giulio Cerullo — Dipartimento di Fisica, Politecnico di Milano, I-20133 Milano, Italy; Department of Chemistry, University of Southern California, Los Angeles, California 90089, United States; orcid.org/0000-0002-9534-2702; Email: giulio.cerullo@polimi.it

Stefano Dal Conte — Dipartimento di Fisica, Politecnico di Milano, I-20133 Milano, Italy; o orcid.org/0000-0001-8582-3185; Email: stefano.dalconte@polimi.it

Authors

Zilong Wang – Dipartimento di Fisica, Politecnico di Milano, I-20133 Milano, Italy

Patrick Altmann – Dipartimento di Fisica, Politecnico di Milano, I-20133 Milano, Italy

Christoph Gadermaier – Dipartimento di Fisica, Politecnico di Milano, I-20133 Milano, Italy; Center for Nano Science and Technology, Italian Institute of Technology, I-20133 Milano, Italy

Yating Yang — College of Chemistry, Key Laboratory of Theoretical and Computational Photochemistry of Ministry of Education, Beijing Normal University, Beijing 100085, P.R. China

Wei Li – Department of Electrical and Computer Engineering, University of Texas at Austin, Austin, Texas 75858, United States

Lavinia Ghirardini — Dipartimento di Fisica, Politecnico di Milano, I-20133 Milano, Italy

Chiara Trovatello — Dipartimento di Fisica, Politecnico di Milano, I-20133 Milano, Italy; orcid.org/0000-0002-8150-9743

Marco Finazzi – Dipartimento di Fisica, Politecnico di Milano, I-20133 Milano, Italy

Lamberto Duò – Dipartimento di Fisica, Politecnico di Milano, I-20133 Milano, Italy Michele Celebrano — Dipartimento di Fisica, Politecnico di Milano, I-20133 Milano, Italy; o orcid.org/0000-0003-3336-3580

Run Long — College of Chemistry, Key Laboratory of Theoretical and Computational Photochemistry of Ministry of Education, Beijing Normal University, Beijing 100085, P.R. China; © orcid.org/0000-0003-3912-8899

Deji Akinwande – Department of Electrical and Computer Engineering, University of Texas at Austin, Austin, Texas 75858, United States; oorcid.org/0000-0001-7133-5586

Complete contact information is available at: https://pubs.acs.org/10.1021/acs.nanolett.0c04955

Notes

The authors declare no competing financial interest.

ACKNOWLEDGMENTS

We acknowledge funding from PRIN 2017 Programme (Prot. 20172H2SC4) from the MIUR, PRIN 2017 NOMEN (Prot. 2017MP7F8F), the support by the European Union Horizon 2020 Programme under Grant Agreement 881603 Graphene Core 3 and the support of the U.S. National Science Foundation Grant CHE-1900510. D.A. acknowledges the Presidential Early Career Award for Scientists and Engineers (PECASE) Grant W911NF-16-1-0277. R.L. acknowledges the National Natural Science Foundation of China, Grant No. 21973006.

REFERENCES

- (1) Chhowalla, M.; Shin, H. S.; Eda, G.; Li, L.-J.; Loh, K. P.; Zhang, H. The Chemistry of Two-Dimensional Layered Transition Metal Dichalcogenide Nanosheets. *Nat. Chem.* **2013**, *5*, 263–275.
- (2) Radisavljevic, B.; Radenovic, A.; Brivio, J.; Giacometti, V.; Kis, A. Single-Layer MoS₂ Transistors. *Nat. Nanotechnol.* **2011**, *6*, 147–150.
- (3) Wang, Q. H.; Kalantar-Zadeh, K.; Kis, A.; Coleman, J. N.; Strano, M. S. Electronics and Optoelectronics of Two-Dimensional Transition Metal Dichalcogenides. *Nat. Nanotechnol.* **2012**, *7*, 699–712.
- (4) Fiori, G.; Bonaccorso, F.; Iannaccone, G.; Palacios, T.; Neumaier, D.; Seabaugh, A.; Banerjee, S. K.; Colombo, L. Electronics Based on Two-Dimensional Materials. *Nat. Nanotechnol.* **2014**, *9*, 768–779.
- (5) Jariwala, D.; Sangwan, V. K.; Lauhon, L. J.; Marks, T. J.; Hersam, M. C. Emerging Device Applications for Semiconducting Two-Dimensional Transition Metal Dichalcogenides. *ACS Nano* **2014**, *8*, 1102–1120.
- (6) Mak, K. F.; Shan, J. Photonics and Optoelectronics of 2D Semiconductor Transition Metal Dichalcogenides. *Nat. Photonics* **2016**, *10*, 216–226.
- (7) Koppens, F. L. H.; Mueller, T.; Avouris, Ph; Ferrari, A. C.; Vitiello, M. S.; Polini, M. Photodetectors based on graphene, other two-dimensional materials and hybrid systems. *Nat. Nanotechnol.* **2014**, *9*, 780–793.
- (8) Palummo, M.; Bernardi, M.; Grossman, J. Exciton radiative lifetimes in two-dimensional transition metal dichalcogenides. *Nano Lett.* **2015**, 15, 2794–2800.
- (9) Robert, C.; Lagarde, D.; Cadiz, F.; Wang, G.; Lassagne, B.; Amand, T.; Balocchi, A.; Renucci, P.; Tongay, S.; Urbaszek, B.; Marie, X. Exciton radiative lifetime in transition metal dichalcogenide monolayers. *Phys. Rev. B: Condens. Matter Mater. Phys.* **2016**, 93, 205423
- (10) Komsa, H.-P.; Krasheninnikov, A. V. Electronic structures and optical properties of realistic transition metal dichalcogenide heterostructures from first principles. *Phys. Rev. B: Condens. Matter Mater. Phys.* **2013**, *88*, No. 085318.

- (11) Amin, B.; Singh, N.; Schwingenschlögl, U. Heterostructures of transition metal dichalcogenides. *Phys. Rev. B: Condens. Matter Mater. Phys.* **2015**, 92, No. 075439.
- (12) Wu, D.; Li, W.; Rai, A.; Wu, X.; Movva, H. C. P.; Yogeesh, M. N.; Chu, Z.; Banerjee, S. K.; Akinwande, D.; Lai, K. Visualization of Local Conductance in MoS₂/WSe₂ Heterostructure Transistors. *Nano Lett.* **2019**, *19*, 1976–1981.
- (13) Hong, X.; Kim, J.; Shi, S.-F.; Zhang, Y.; Jin, C.; Sun, Y.; Tongay, S.; Wu, J.; Zhang, Y.; Wang, F. Ultrafast Charge Transfer in Atomically Thin MoS₂/WS₂ Heterostructures. *Nat. Nanotechnol.* **2014**, *9*, 682–686.
- (14) Ceballos, F.; Bellus, M. Z.; Chiu, H.-Y.; Zhao, H. Ultrafast Charge Separation and Indirect Exciton Formation in a MoS₂-MoSe₂ Van Der Waals Heterostructure. ACS Nano **2014**, *8*, 12717–12724.
- (15) Pan, S.; Ceballos, F.; Bellus, M. Z.; Zereshki, P.; Zhao, H. Ultrafast charge transfer between MoTe₂ and MoS₂ monolayers. 2D *Mater.* **2017**, 4, No. 015033.
- (16) Ceballos, F.; Ju, M.-G.; Lane, S. D.; Zeng, X. C.; Zhao, H. Highly Efficient and Anomalous Charge Transfer in van der Waals Trilayer Semiconductors. *Nano Lett.* **2017**, *17*, 1623–1628.
- (17) Xu, W.; Liu, W.; Schmidt, J. F.; Zhao, W.; Lu, X.; Raab, T.; Diederichs, C.; Gao, W.; Seletskiy, D. V.; Xiong, Q. Correlated fluorescence blinking in two-dimensional semiconductor heterostructures. *Nature* **2017**, *541*, 62–67.
- (18) Zhu, H.; Wang, J.; Gong, Z.; Kim, Y. D.; Hone, J.; Zhu, X.-Y. Interfacial Charge Transfer Circumventing Momentum Mismatch at Two-Dimensional van der Waals Heterojunctions. *Nano Lett.* **2017**, *17*, 3591–3598.
- (19) Ji, Z.; Hong, H.; Zhang, J.; Zhang, Q.; Huang, W.; Cao, T.; Qiao, R.; Liu, C.; Liang, J.; Jin, C.; Jiao, L.; Shi, K.; Meng, S.; Liu, K. Robust Stacking-Independent Ultrafast Charge Transfer in MoS₂/WS₂ bilayers. ACS Nano 2017, 11, 12020–12026.
- (20) Jin, C.; Ma, E. Y.; Karni, O.; Regan, E. C.; Wang, F.; Heinz, T. F. Ultrafast Dynamics in Van Der Waals Heterostructures. *Nat. Nanotechnol.* **2018**, *13*, 994–1003.
- (21) Liu, F.; Li, Q.; Zhu, X.-Y. Direct determination of momentum-resolved electron transfer in the photoexcited van der Waals heterobilayer WS₂/MoS₂. *Phys. Rev. B: Condens. Matter Mater. Phys.* **2020**, *101*, 201405.
- (22) Cheng, R.; Li, D.; Zhou, H.; Wang, C.; Yin, A.; Jiang, S.; Liu, Y.; Chen, Y.; Huang, Y.; Duan, X. Electroluminescence and Photocurrent Generation From Atomically Sharp WSe₂/MoS₂ heterojunction p—n diodes. *Nano Lett.* **2014**, *14*, 5590—5597.
- (23) Pospischil, A.; Furchi, M. M.; Mueller, T. Solar-Energy Conversion and Light Emission in an Atomic Monolayer p—n Diode. *Nat. Nanotechnol.* **2014**, *9*, 257–261.
- (24) Lee, C.-H.; Lee, G.-H.; van der Zande, A. M.; Chen, W.; Li, Y.; Han, M.; Cui, X.; Arefe, G.; Nuckolls, C.; Heinz, T. F.; Guo, J.; Hone, J.; Kim, P. Atomically Thin p—n Junctions with Van Der Waals Heterointerfaces. *Nat. Nanotechnol.* **2014**, *9*, 676—681.
- (25) Shi, J.; Tong, R.; Zhou, X.; Gong, Y.; Zhang, Z.; Ji, Q.; Zhang, Y.; Fang, Q.; Gu, L.; Wang, X.; Liu, Z.; Zhang, Y. Temperature-Mediated Selective Growth of MoS₂/WS₂ and WS₂/MoS₂ Vertical Stacks on Au Foils for Direct Photocatalytic Applications. *Adv. Mater.* **2016**, 28, 10664–10672.
- (26) Pesci, F. M.; Sokolikova, M. S.; Grotta, C.; Sherrell, P. C.; Reale, F.; Sharda, K.; Ni, N.; Palczynski, P.; Mattevi, C. MoS₂/WS₂ Heterojunction for Photoelectrochemical Water Oxidation. *ACS Catal.* **2017**, *7*, 4990–4998.
- (27) Rivera, P.; Schaibley, J. R.; Jones, A. R.; Ross, J. S.; Wu, S.; Aivazian, G.; Klement, P.; Seyler, K.; Clark, G.; Ghimire, N. J.; Yan, J.; Mandrus, D. G.; Yao, W.; Xu, X. Observation of Long-Lived Interlayer Excitons in Monolayer MoSe₂/WSe₂ Heterostructures. *Nat. Commun.* **2015**, *6*, 6242.
- (28) Miller, B.; Steinhoff, A.; Pano, B.; Klein, J.; Jahnke, F.; Holleitner, A.; Wurstbauer, U. Long-Lived Direct and Indirect Interlayer Excitons in van der Waals Heterostructures. *Nano Lett.* **2017**, *17*, 5229–5237.

- (29) Nagler, P.; Plechinger, G.; Ballottin, M. V.; Mitioglu, A.; Meier, S.; Paradiso, N.; Strunk, C.; Chernikov, A.; Christianen, P. C. M.; Schüller, C.; Korn, T. Interlayer Exciton Dynamics in a Dichalcogenide Monolayer Heterostructure. 2D Mater. 2017, 4, No. 025112.
- (30) Unuchek, D.; Ciarrocchi, A.; Avsar, A.; Watanabe, K.; Taniguchi, T.; Kis, A. Room-Temperature Electrical Control of Exciton Flux in a van der Waals Heterostructure. *Nature* **2018**, *560*, 340–344.
- (31) Yuan, L.; Zheng, B.; Kunstmann, J.; Brumme, T.; Kuc, A. B.; Ma, C.; Deng, S.; Blach, D.; Pan, A.; Huang, L. Twist-Angle-Dependent Interlayer Exciton Diffusion in WS₂–WSe₂ heterobilayers. *Nat. Mater.* **2020**, *19*, 617–623.
- (32) Jin, C.; Kim, J.; Utama, M. I. B.; Regan, E. C.; Kleemann, H.; Cai, H.; Shen, Y.; Shinner, M. J.; Sengupta, A.; Watanabe, K.; Taniguchi, T.; Tongay, S.; Zettl, A.; Wang, F. Imaging of Pure Spin-Valley Diffusion Current in WS₂-WSe₂ Heterostructures. *Science* **2018**, *360*, 893–896.
- (33) Unuchek, D.; Ciarrocchi, A.; Avsar, A.; Sun, Z.; Watanabe, K.; Taniguchi, T.; Kis, A. Valley-polarized Exciton Currents in a van der Waals Heterostructure. *Nat. Nanotechnol.* **2019**, *14*, 1104–1109.
- (34) Zhang, N.; Surrente, A.; Baranowski, M.; Maude, D. K.; Gant, P.; Castellanos-Gomez, A.; Plochocka, P. Moiré Intralayer Excitons in a MoSe₂/MoS₂ Heterostructure. *Nano Lett.* **2018**, *18*, 7651–7657.
- (35) Seyler, K. L.; Rivera, P.; Yu, H.; Wilson, N. P.; Ray, E. L.; Mandrus, D. G.; Yan, J.; Yao, W.; Xu, X. Signatures of Moiré-trapped Valley Excitons in MoSe₂/WSe₂ Heterobilayers. *Nature* **2019**, 567, 66–70.
- (36) Tran, K.; et al. Evidence for Moiré excitons in van der Waals Heterostructures. *Nature* **2019**, *567*, 71–75.
- (37) Jin, C.; Regan, E. C.; Yan, A.; Iqbal Bakti Utama, M.; Wang, D.; Zhao, S.; Qin, Y.; Yang, S.; Zheng, Z.; Shi, S.; Watanabe, K.; Taniguchi, T.; Tongay, S.; Zettl, A.; Wang, F. Observation of Moiré Excitons in WSe₂/WS₂ Heterostructure Superlattices. *Nature* **2019**, 567, 76–80.
- (38) Alexeev, E. M.; Ruiz-Tijerina, D. A.; Danovich, M.; Hamer, M. J.; Terry, D. J.; Nayak, P. K.; Ahn, S.; Pak, S.; Lee, J.; Sohn, J. I.; Molas, M. R.; Koperski, M.; Watanabe, K.; Taniguchi, T.; Novoselov, K. S.; Gorbachev, R. V.; Shin, H. S.; Fal'ko, W. I.; Tartakovskii, A. I. Resonantly Hybridized Excitons in Moiré Superlattices in van der Waals Heterostructures. *Nature* **2019**, *567*, 81–86.
- (39) Dal Conte, S.; Trovatello, C.; Gadermaier, C.; Cerullo, G. Ultrafast Photophysics of 2D Semiconductors and Related Heterostructures. *Trends Chem.* **2020**, *2*, 28–42.
- (40) Wang, H.; Bang, J.; Sun, Y.; Liang, L.; West, D.; Meunier, V.; Zhang, S. The Role of Collective Motion in the Ultrafast Charge Transfer in van der Waals Heterostructures. *Nat. Commun.* **2016**, *7*, 11504
- (41) Li, L.; Long, R.; Prezhdo, O. V. Charge Separation and Recombination in Two-Dimensional MoS₂/WS₂: Time-Domain *Ab Initio* Modeling. *Chem. Mater.* **2017**, 29, 2466–2473.
- (42) Long, R.; Prezhdo, O. V. Quantum Coherence Facilitates Efficient Charge Separation at a $MoS_2/MoSe_2$ van der Waals Junction. *Nano Lett.* **2016**, *16*, 1996–2003.
- (43) Zheng, Q.; Saidi, W. A.; Xie, Y.; Lan, Z.; Prezhdo, O. V.; Petek, H.; Zhao, J. Phonon-Assisted Ultrafast Charge Transfer at Van Der Waals Heterostructure Interface. *Nano Lett.* **2017**, *17*, 6435–6442.
- (44) Zhang, J.; Hong, H.; Lian, C.; Ma, W.; Xu, X.; Zhou, X.; Fu, H.; Liu, K.; Meng, S. Interlayer-State-Coupling Dependent Ultrafast Charge Transfer in MoS₂/WS₂ bilayers. *Adv. Sci.* **2017**, *4*, 1700086.
- (45) Zheng, Q.; Xie, Y.; Lan, Z.; Prezhdo, O. V.; Saidi, W. A.; Zhao, J. Phonon-Coupled Ultrafast Interlayer Charge Oscillation at van der Waals Heterostructure Interfaces. *Phys. Rev. B: Condens. Matter Mater. Phys.* **2018**, *97*, 205417.
- (46) Ovesen, S.; Brem, S.; Linderälv, C.; Kuisma, M.; Korn, T.; Erhart, P.; Selig, M.; Malic, M. Interlayer Exciton Dynamics in van der Waals Heterostructures. *Commun. Phys.* **2019**, *2*, 23.

- (47) Liu, J.; Zhang, X.; Lu, G. Excitonic Effect Drives Ultrafast Dynamics in van der Waals Heterostructures. *Nano Lett.* **2020**, 20, 4631–4637.
- (48) Wang, Y.; Wang, Z.; Yao, W.; Liu, G.-B.; Yu, H. Interlayer Coupling in Commensurate and Incommensurate Bilayer Structures of Transition-Metal Dichalcogenides. *Phys. Rev. B: Condens. Matter Mater. Phys.* **2017**, 95, 115429.
- (49) Raja, A.; Chaves, A.; Yu, J.; Arefe, G.; Hill, H. M.; Rigosi, A. F.; Berkelbach, T. C.; Nagler, P.; Schüller, C.; Korn, T.; Nuckolls, C.; Hone, J.; Brus, L. E.; Heinz, T. F.; Reichman, D. R.; Chernikov, A. Coulomb Engineering of the Bandgap and Excitons in Two-Dimensional Materials. *Nat. Commun.* **2017**, *8*, 15251.
- (50) Pogna, E. A. A.; Marsili, M.; De Fazio, D.; Dal Conte, S.; Manzoni, C.; Sangalli, D.; Yoon, D.; Lombardo, A.; Ferrari, A. C.; Marini, A.; Cerullo, G.; Prezzi, D. Photo-Induced Bandgap Renormalization Governs the Ultrafast Response of Single-Layer MoS₂. ACS Nano **2016**, 10, 1182–1188.
- (51) Cunningham, P. D.; Hanbicki, A. T.; McCreary, K. M.; Jonker, B. T. Photoinduced Bandgap Renormalization and Exciton Binding Energy Reduction in WS₂. ACS Nano **2017**, 11, 12601–12608.
- (52) Zhou, H.; Zhao, Y.; Zhu, H. Dielectric Environment-Robust Ultrafast Charge Transfer Between Two Atomic Layers. *J. Phys. Chem. Lett.* **2019**, *10*, 150–155.
- (53) Chernikov, A.; Ruppert, C.; Hill, H. M.; Rigosi, A. F.; Heinz, T. F. Population Inversion and Giant Bandgap Renormalization in Atomically thin WS, layers. *Nat. Photonics* **2015**, *9*, 466–470.
- (54) Craig, C. F.; Duncan, W. R.; Prezhdo, O. V. Trajectory Surface Hopping in the Time-Dependent Kohn-Sham Approach For Electron-Nuclear Dynamics. *Phys. Rev. Lett.* **2005**, *95*, 163001.
- (55) Jaeger, H. M.; Fischer, S.; Prezhdo, O. V. Decoherence-Induced Surface Hopping. J. Chem. Phys. 2012, 137, 22A545.
- (56) Long, R.; Prezhdo, O. V.; Fang, W. Nonadiabatic Charge Dynamics in Novel Solar Cell Materials. *Wiley Interdiscip. Rev. Comput. Mol. Sci.* **2017**, *7*, e1305.
- (57) Zhang, F.; Li, W.; Dai, X. Q. Modulation of Electronic Structures of MoSe₂/WSe₂ Van Der Waals Heterostructure by External Electric Field. *Solid State Commun.* **2017**, *266*, 11–15.
- (58) Terrones, H.; Lopez-Urias, F.; Terrones, M. Novel Hetero-Layered Materials with Tunable Direct Band Gaps by Sandwiching Different Metal Disulfides and Diselenides. *Sci. Rep.* **2013**, *3*, 1549.
- (59) Li, L. Q.; Long, R.; Prezhdo, O. V. Charge Separation and Recombination in Two-Dimensional MoS₂/WS₂: Time-Domain Ab Initio Modeling. *Chem. Mater.* **2017**, *29*, 2466–2473.
- (60) O'Brien, M.; McEvoy, N.; Hanlon, D.; Hallam, T.; Coleman, J. N.; Duesberg, G. S. Mapping of Low-Frequency Raman Modes in Cvd-Grown Transition Metal Dichalcogenides: Layer Number, Stacking Orientation and Resonant Effects. Sci. Rep. 2016, 6, 19476.
- (61) Wang, H.; Zhang, C.; Rana, F. Ultrafast Dynamics of Defect-Assisted Electron-Hole Recombination in Monolayer MoS₂. *Nano Lett.* **2015**, *15*, 339–345.
- (62) Zhang, X.-X.; You, Y.; Yang, S.; Zhao, F.; Heinz, T. F. Experimental Evidence for Dark Excitons in Monolayer WSe₂. *Phys. Rev. Lett.* **2015**, *115*, 257403.